HYDROGEN EMBRITTLEMENT IN NICKEL-BASED ALLOYS:

AN ABRIDGED SAMPLE THESIS TO ILLUSTRATE

FORMATTING GUIDELINES

by

Michelle N. Kent

A thesis submitted to the Faculty and the Board of Trustees of the Colorado School of Mines in partial fulfillment of the requirements for the degree of Master of Science (Metallurgical and Materials Engineering).

Golden, Colorado

Date _____

Signed: _____

Michelle N. Kent

Signed: _____

Dr. Kip O. Findley
Thesis Advisor

Golden, Colorado

Date _____

Signed: _____

Dr. Ivar Reimanis
Professor and Department Head
Metallurgical and Materials Engineering

ABSTRACT

During heat treatment, the thermal history can vary across a thick section of bar or forged product, resulting in a variation in mechanical properties, including hydrogen embrittlement (HE) susceptibility in Ni-base alloys. While it is well-established that δ phase precipitation occurs along grain boundaries in Alloy 718, it is unclear how much δ phase is necessary to diminish the HE resistance. Alloy 945X was designed to improve the HE resistance relative to Alloy 718 by avoiding δ phase precipitation; however, $M_{23}C_6$ carbides can form along grain boundaries in Alloy 945X under typical aging conditions. This work investigates the HE susceptibilities of Alloys 718 and 945X conditions aged at industrially-relevant temperatures that span the δ and $M_{23}C_6$ precipitation thresholds, respectively. The first objective of the study was to determine the sensitivity of HE susceptibility to small amounts of δ phase in Alloy 718. The second objective was to determine whether $M_{23}C_6$ phase increased the HE susceptibility, as the effects of $M_{23}C_6$ on HE susceptibility are not well established. Thirdly, the effects of δ and $M_{23}C_6$ were compared to determine whether $M_{23}C_6$ was as deleterious to HE resistance as δ phase. For hydrogen embrittlement testing, incremental step load tests were performed with circular notched tensile specimens subjected to *in situ* cathodic charging while crack initiation and growth were monitored using the direct current potential drop technique. For conditions with similar hardness values that spanned the δ precipitation threshold, fine, infrequent, and discontinuous δ phase precipitation resulted in an increase in HE susceptibility and increasingly intergranular fracture morphology, indicating that even a small amount of δ can reduce the HE resistance. The HE susceptibility also increased with $M_{23}C_6$ precipitation and growth in Alloy 945X conditions with similar hardness. The Alloy 945X conditions with $M_{23}C_6$ contained more frequent and more continuous grain boundary precipitates than the Alloy 718 conditions that contained δ phase; however, the HE susceptibility of $M_{23}C_6$-containing Alloy 945X was similar to the HE susceptibility of δ-containing Alloy 718, suggesting that $M_{23}C_6$ is not as deleterious to HE susceptibility as δ phase, though both phases significantly reduce the HE resistance. Increasing HE susceptibility correlates with decreasing Charpy impact toughness, likely because grain boundary precipitates diminish both of these properties.

TABLE OF CONTENTS

LIST OF FIGURES

LIST OF TABLES

ACKNOWLEDGEMENTS

Selected components of a thesis prepared in Spring 2022 by Michelle Kent have been included in this document to illustrate the Thesis Formatting Guidelines of the Office of Graduate Studies (OGS) at the Colorado School of Mines. OGS greatly appreciates Michelle's contribution to developing this sample thesis to assist current and future graduate students.

A standard Acknowledgements section of a Mines thesis typically includes the following types of statements, as applicable:

I would like to acknowledge the support of [Advisor] and committee members [XX, YY, ZZ] as well as key collaborators [AA, BB, CC]. Funding was provided by [XX, YY]. Lab facilities at [XXXX] were used in the work described in Chapter X. I also appreciate the contributions of [AA, BB, CC, DD] to this project.

Dedication: Optional. Place here at center of page if included.

CHAPTER 1
INTRODUCTION

Precipitation hardenable Ni-Fe-Cr corrosion resistant alloys (CRAs) are used for downhole oil and gas components such as valves, packer assemblies, hangers, and drill tools, because they exhibit a favorable combination of high strength, high toughness, and good corrosion resistance. CRAs are often subjected to cathodic protection during service to improve corrosion resistance, which attracts hydrogen to the surface of the cathode. The presence of hydrogen, when combined with a tensile stress on a susceptible material, can lead to brittle failure in normally-ductile materials, a phenomenon known as hydrogen embrittlement (HE).

1.1 Research Objectives and Questions

The objective of this project was to investigate the effect of different degrees of grain boundary precipitation on the HE susceptibility of the selected Ni-base alloys. Additionally, the HE testing results were compared to hydrogen-free mechanical properties to find correlations that could be indicators of the material's performance in hydrogen. The following questions were developed to address the objectives of this research.

1. *How does a small amount of δ phase precipitation affect the HE susceptibility of Alloy 718?* It was hypothesized that even small amounts of δ phase might diminish the HE resistance, but that this phenomenon is often convoluted by the improved HE resistance from overaging γ" precipitates as δ phase forms. To study the HE sensitivity to small amounts of δ phase, Alloy 718 was heat treated for a series of industrially-relevant times and temperatures that spanned the δ precipitation threshold while maintaining similar hardness between conditions. HE susceptibility and fracture morphology were compared between conditions with different amounts of δ phase.
2. *How does $M_{23}C_6$ precipitation affect HE susceptibility in Alloy 945X?* While several studies have investigated the HE susceptibility of Alloy 945X, none have reported the effect of $M_{23}C_6$ precipitation on HE susceptibility during long aging times at industrially-relevant temperatures. Since $M_{23}C_6$ is a grain boundary phase similar to δ, it is possible that $M_{23}C_6$ could also diminish the HE resistance. As in Alloy 718, the HE

sensitivity to $M_{23}C_6$ was investigated by heat treating Alloy 945X for times spanning the $M_{23}C_6$ precipitation threshold at an industrially-relevant temperature while maintaining similar hardness between conditions, and the HE susceptibility and fracture morphology were compared between conditions.

1.2 Thesis Overview and Physical Metallurgy of Alloy 718 and Alloy 945X for Oil and Gas Applications

An introduction to the alloys used in this study and a review of previous hydrogen embrittlement investigations that establish the foundation for this research are presented in Chapter 2. The experimental procedure described in Chapter 3 begins with an explanation of the heat treatment selection process, followed by details of the hardness, tensile, and Charpy impact testing methods and the hydrogen embrittlement testing and characterization procedures. The results from testing and characterization are presented in Chapter 4. The ISL testing results are presented as the stress intensity factor for unstable crack growth (K_u) and the ratio of the load at which unstable crack growth initiated under cathodic charging to the peak load reached in quasi-static tensile tests for CNT specimens tested in ambient air. Figure 1.1(a) shows a scanning electron microscope (SEM) image of spherical γ' and ellipsoidal γ" precipitates in a matrix, and Figure 1.1(b) shows δ phase precipitates along the grain boundary.

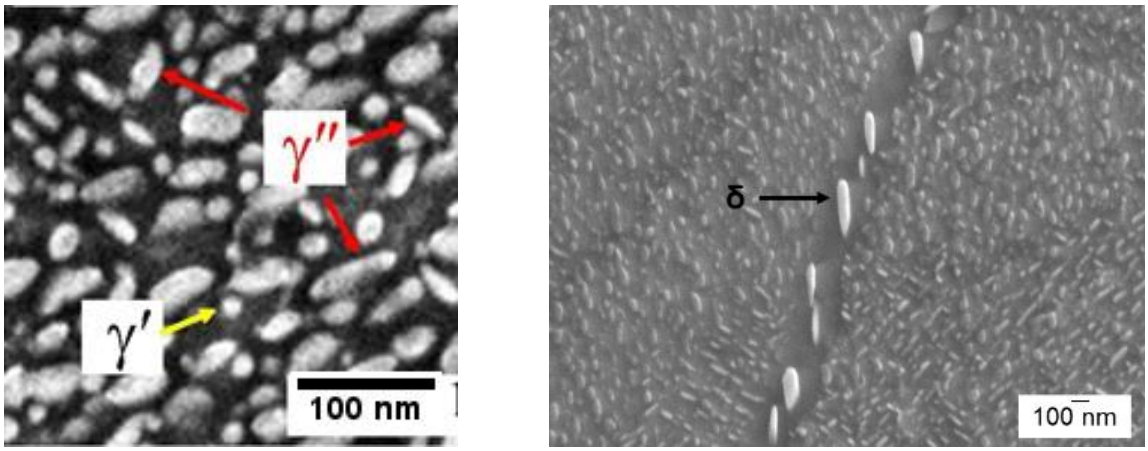

(a) (b)

Figure 1.1 Scanning electron micrographs (SEM) of (a) γ' and γ" precipitates in the matrix of Alloy 718 aged at 780 °C for 8 h and (b) δ phase along the grain boundary in Alloy 718 aged at 750 °C for 20 h [20].

The time-temperature-transformation (TTT) diagrams for Alloy 718 and Alloy 945X are shown in Figure 1.2(a) and (b), respectively [21,22]. The Alloy 718 TTT diagram is overlaid with the API Standard 6ACRA heat treatment time and temperature ranges for the 965 MPa heat treatment (blue) and the first step of the 1034 MPa heat treatment (green). The Alloy 945X TTT diagram is overlaid with the API Standard 6ACRA heat treatment time and temperature range for the first step of the 965 MPa heat treatment (yellow).

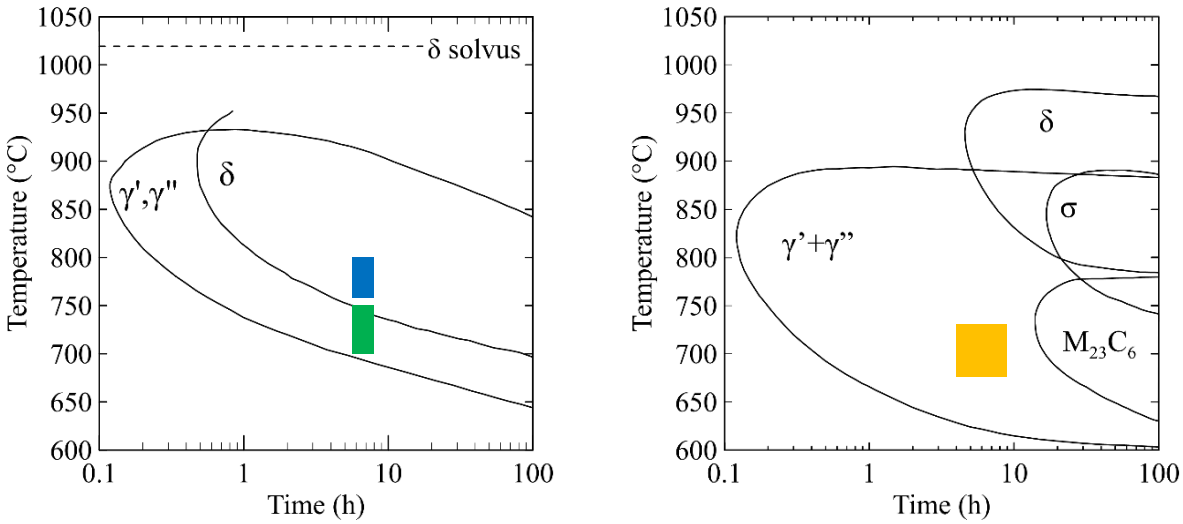

Figure 1.2 TTT diagrams for (a) Alloy 718 and (b) Alloy 945X [7].

It was hypothesized that even small amounts of δ phase might diminish the HE resistance, but that this phenomenon is often convoluted by the improved HE resistance from overaging γ" precipitates as δ phase forms. To study the HE sensitivity to small amounts of δ phase, Alloy 718 was heat treated for a series of industrially-relevant times and temperatures that spanned the δ precipitation threshold while maintaining similar hardness between conditions. HE susceptibility and fracture morphology were compared between conditions with different amounts of δ phase.

CHAPTER 2
PHYSICAL METALLURGY OF HYDROGEN EMBRITTLEMENT-SUSCEPTIBLE ALLOY 718 AND ALLOY 945X FOR OIL AND GAS APPLICATIONS

This chapter discusses the development of Alloy 718 and Alloy 945X for oil and gas applications. The physical metallurgy of these alloys with different heat treatment conditions and precipitation morphologies is reviewed. Hydrogen embrittlement in Ni-base CRAs is discussed in terms of precipitate effects and hydrogen trapping.

2.1 Physical Metallurgy of Alloy 718 and Alloy 945X for Oil and Gas Applications

Relative to the Alloy 718 composition used in gas turbine applications, the minimum Ti and Al concentrations are increased to stabilize intragranular precipitates in the matrix. The C and P concentrations are restricted to improve the toughness. The solution and aging treatments described for Alloy 718 and Alloy 945X in API Standard 6ACRA, Addendum 3 are shown in Table 2.1 [9]. The annealing temperature is increased above 1021 °C for Alloy 718 used in oil and gas applications to improve the fracture toughness and reduce δ phase, a grain boundary phase that is desirable for creep resistance but reduces toughness and HE resistance [3]. The heat treatment used for oil and gas applications typically produces an overaged microstructure, which limits the hardness and is easier to reproduce than an underaged condition for a given hardness.

Table 2.1 Recommended annealing and aging heat treatments described in API Standard 6ACRA [9]

UNS	Minimum Yield Strength	Solution Annealing		Age Hardening
		Temperature (°C)	Time (h)	
N07718	965 MPa (140 ksi)	1021 – 1052 °C	1 – 2.5	760 – 802 °C for 6 – 8 h
N07718	1034 MPa (150 ksi)	1021 – 1052 °C	1 – 2.5	700 – 750 °C for 6 – 8 h, furnace cool to 600 – 650 °C and hold for 6 – 8 h
N09946	965 MPa (140 ksi)	996 – 1066 °C	0.5-4	677 – 732 °C for 4 – 9 h, furnace cool to 600 – 643 °C and hold for 12 h total

Table 2.2 provides a summary of the γ’, γ”, δ, and $M_{23}C_6$ properties. Other precipitates that can form include niobium carbides (NbC), titanium nitrides (TiN), titanium carbides (TiC), Laves phase, and metal carbides (M_6C, M_7C_3).

Table 2.2 δ precipitate condition and Charpy impact toughness for several conditions reported by Kagay [38]

Aging Condition	δ Observed	Impact Toughness at -10 °C (J)
Under-aged	No δ	183 ± 3
Peak-aged	Small δ precipitates along some grain boundaries	112 ± 3
Over-aged	δ were much larger and observed along more grain boundaries	85 ± 2
High δ	δ were large and frequent, extending into grains at many grain boundaries	60 ± 1
Under-aged	No δ	183 ± 3
Peak-aged	Small δ precipitates along some grain boundaries	112 ± 3
Over-aged	δ were much larger and observed along more grain boundaries	85 ± 2
High δ	δ were large and frequent, extending into grains at many grain boundaries	60 ± 1
Under-aged	No δ	183 ± 3
Peak-aged	Small δ precipitates along some grain boundaries	112 ± 3
Over-aged	δ were much larger and observed along more grain boundaries	85 ± 2
High δ	δ were large and frequent, extending into grains at many grain boundaries	60 ± 1
Under-aged	No δ	183 ± 3
Peak-aged	Small δ precipitates along some grain boundaries	112 ± 3
Over-aged	δ were much larger and observed along more grain boundaries	85 ± 2
High δ	δ were large and frequent, extending into grains at many grain boundaries	60 ± 1
Under-aged	No δ	183 ± 3
Peak-aged	Small δ precipitates along some grain boundaries	112 ± 3
Over-aged	δ were much larger and observed along more grain boundaries	85 ± 2
Under-aged	No δ	183 ± 3

Table 2.2 continued

Under-aged	No δ	183 ± 3
Peak-aged	Small δ precipitates along some grain boundaries	112 ± 3
Over-aged	δ were much larger and observed along more grain boundaries	85 ± 2
High δ	δ were large and frequent, extending into grains at many grain boundaries	60 ± 1

The time-temperature-transformation (TTT) diagrams for Alloy 718 and Alloy 945X are shown in Figure 1.2(a) and (b), respectively [21,22]. The TTT diagrams were generated experimentally from the respective alloys and reported in literature; however, small compositional differences within the allowable ranges for the alloys can shift the precipitation curves [21,23,24]. The Alloy 718 TTT diagram is overlaid with the API Standard 6ACRA heat treatment time and temperature ranges for the 965 MPa heat treatment (blue) and the first step of the 1034 MPa heat treatment (green). The Alloy 945X TTT diagram is overlaid with the API Standard 6ACRA heat treatment time and temperature range for the first step of the 965 MPa heat treatment (yellow). In Alloy 718, γ' and γ" precipitate within the first hour during aging between 750 °C and 920 °C, followed by δ phase precipitation. In Alloy 945X, the nose of the γ' and γ" precipitation curve is slightly lower in temperature but generally follows the same behavior as in Alloy 718. The δ precipitation curve is delayed to longer times and higher temperatures in Alloy 945X. $M_{23}C_6$ carbide precipitation is more likely than δ phase formation at times and temperatures typical of heat treating. In thick sections of bar that cool slowly and remain at the elevated aging temperature for a longer duration than the applied heat treatment, it is possible that $M_{23}C_6$ could precipitate during standard heat treatments.

2.1.1 γ' and γ" Precipitation in Ni-base Alloys

γ' and γ" nucleation occurs within minutes spent at typical aging temperatures. Since the cubic γ' and tetragonal γ" crystal symmetries are similar to that of the FCC matrix, precipitates form when lattice positions in the matrix are replaced with the ordered atomic arrangement of the precipitate lattice [14]. Thus, coherency is maintained between the matrix and the precipitates during precipitation and growth. The γ' and γ" precipitates both nucleate homogeneously in the γ matrix under most circumstances.

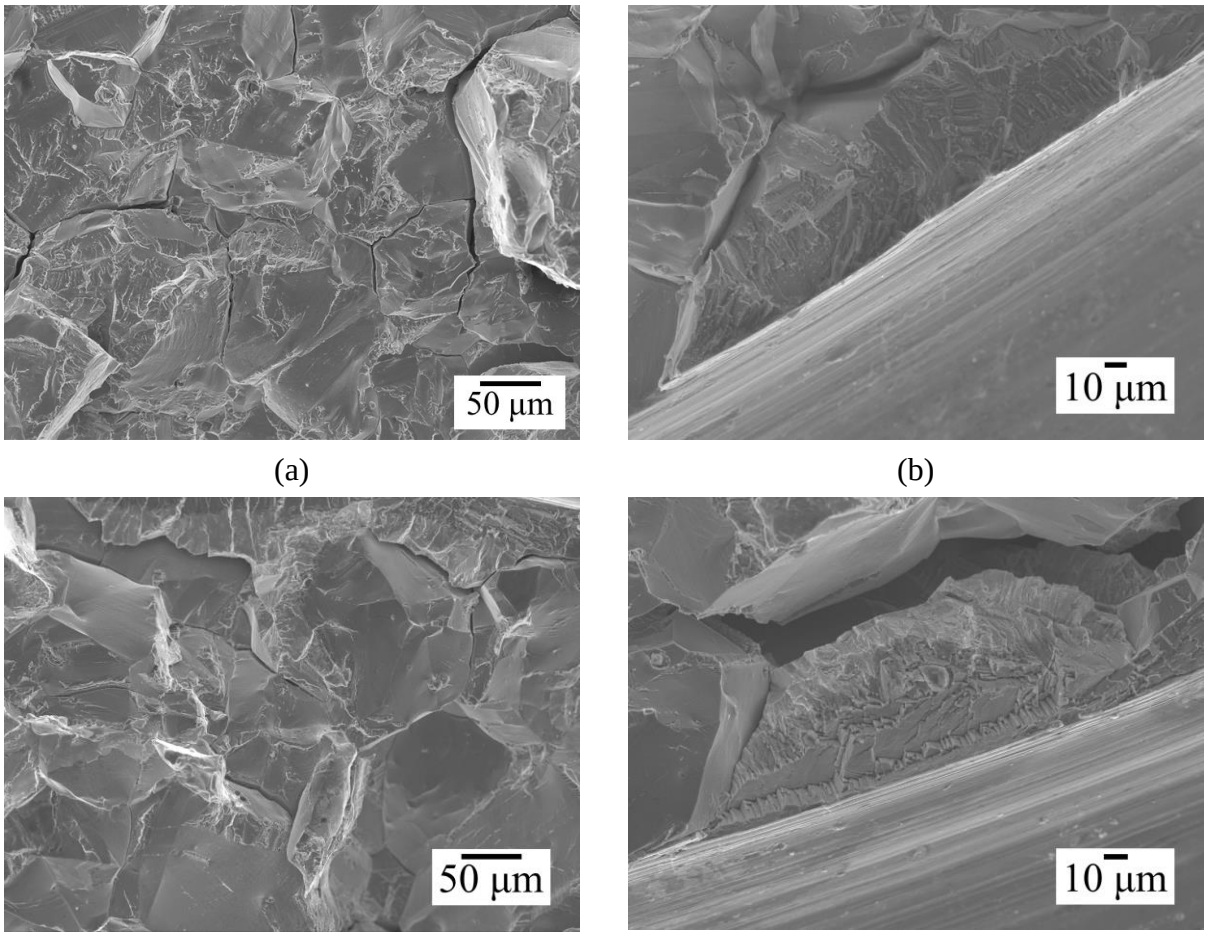

Figure 2.1 Fracture surfaces in the hydrogen-affected region of Alloy 718 CNT specimens aged at 750 °C for 6 h (a) away from the notch and (b) near the notch, 12 h (c) away from the notch and (d) near the notch.

Figure 2.2 SEM-EDS map of δ phase indicated in the micrograph in (a) in Alloy 718 heat treated at 750 °C for 20 h. SEM-EDS heat maps are shown for (b) Al, (c) C, (d) Cr, (e) Fe, (f) Nb, (g) Ni, and (h) Ti. The colors correspond to the count intensity scale in (a). Room temperature Charpy impact toughness plotted as a function of weight percent $M_{23}C_6$ in test alloy C-HRA-2 [43]. Conditions in which $M_{23}C_6$ was observed only in the matrix and both in the matrix and along grain boundaries are noted

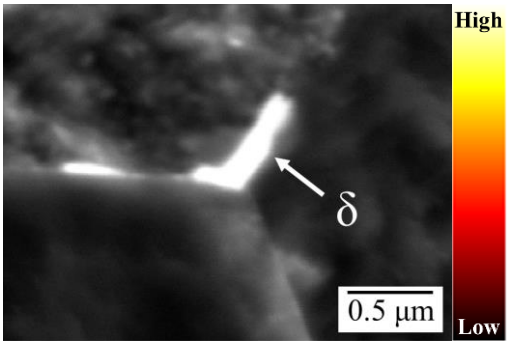
High
δ
0.5 μm
Low

(a)

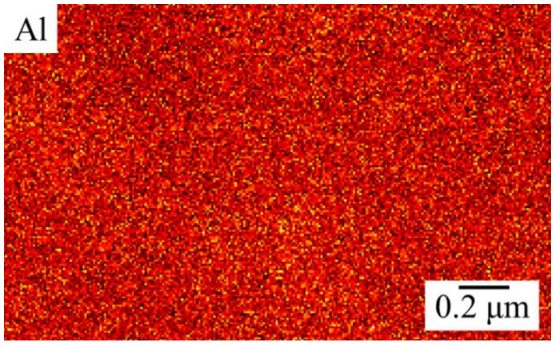
Al
0.2 μm

(b)

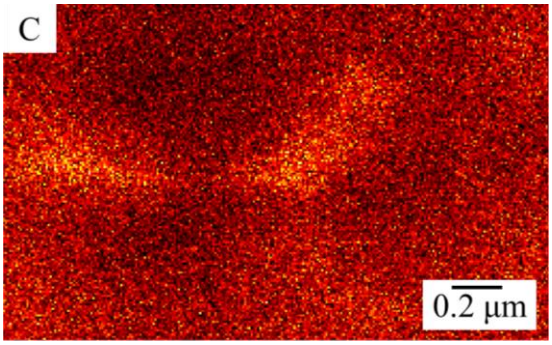
C
0.2 μm

(c)

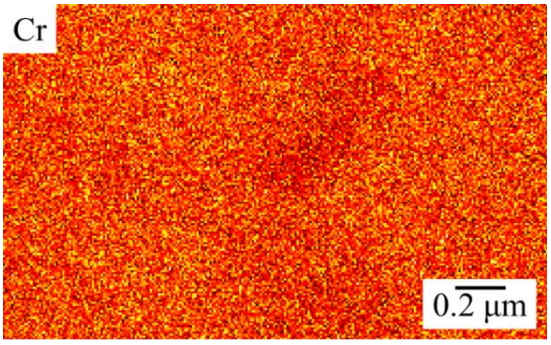
Cr
0.2 μm

(d)

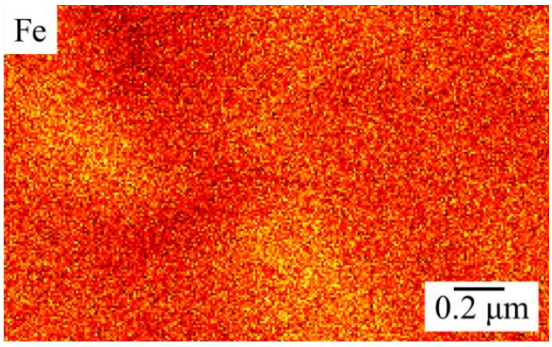
Fe
0.2 μm

(e)

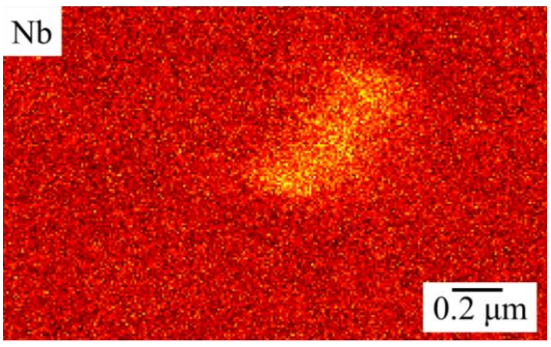
Nb
0.2 μm

(f)

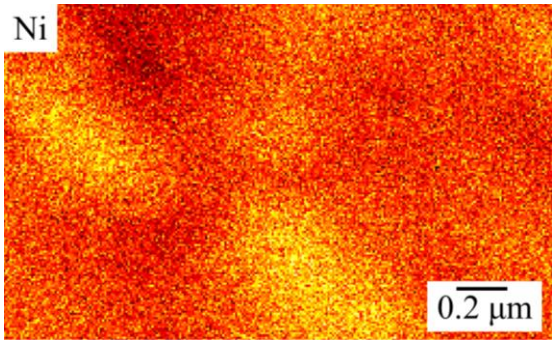
Ni
0.2 μm

(g)

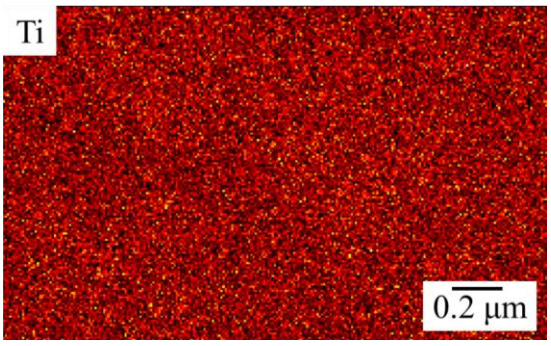
Ti
0.2 μm

(h)

CHAPTER 3

EFFECT OF DELTA PHASE ON THE HYDROGEN EMBRITTLEMENT SUSCEPTIBLITY OF ALLOY 718

Based on a paper published in the *Journal of Abridged Theses**

Michelle Kent[1], Kip Findley[1], John Doe[2], Jane Collaborator[3]

3.1 Abstract

The objective of this project was to investigate changes in hydrogen embrittlement susceptibility with heat treatment conditions for Alloy 718 and Alloy 945X within the parameters of API Standard 6ACRA. Previous work by Kagay investigated the effects of aging condition on the HE susceptibility of Alloy 718 [53]. This study applied the same HE evaluation technique to industrially-relevant aging conditions. An initial heat treatment investigation was conducted for both alloys to select conditions for the subsequent HE investigation. The objective of this initial survey was to identify conditions with comparable hardness in Alloy 718 and $M_{23}C_6$ formation in Alloy 945X. A similar hardness was sought to avoid strength-related effects causing differences in HE susceptibility between conditions, as strength typically correlates with HE susceptibility [52,75]. Heat treatment times and temperatures were selected near the range specified in API Standard 6ACRA [9]. For Alloy 718, the aging temperature range is 700 to 750 °C, and for Alloy 945X the range is 677 to 732 °C.

3.2 Introduction

Alloy 718 and 945X were received as 19.1 mm (0.75 in) lab-produced hot-rolled plate approximately 10 cm (4 in) in width. The stress intensity factor for unstable crack growth, K_u, is calculated from the load *P* at which unstable crack growth occurs using Equation 3.1 [83],

$$K_u = \frac{P}{\pi(d-a)^2}\sqrt{\pi(d-a)}F \tag{3.1}$$

[1]Colorado School of Mines, Metallurgical and Materials Engineering
[2]National Aeronautics and Space Administration (NASA), Materials Research and Technology
[3]National Renewable Energy Laboratory (NREL), Analytical Microscopy and Imaging Science
*See Appendix B for permission and citation

where *d* is the notch radius, *a* is the crack length, *D* is the unnotched radius, and *F* is given by Equation 3.2,

$$F = \sqrt{1 - \left(\frac{d-a}{D}\right)} * \frac{1}{2} * \left[1 + \frac{1}{2}\left(\frac{d-a}{D}\right) + \frac{3}{8}\left(\frac{d-a}{D}\right)^2 - 0.363\left(\frac{d-a}{D}\right)^3 + 0.731\left(\frac{d-a}{D}\right)^4\right] \quad (3.2)$$

The alloy compositions are shown in Table 3.1.

Table 3.1 Chemical composition of selected Ni-base alloy grades (wt pct)

wt pct	Ni	Fe	Cr	Nb	Mo	Ti	Al	Co
Alloy 718	53.30	17.90	18.5	5.07	2.88	1.01	0.52	0.20
Alloy 945X	53.60	14.30	20.50	4.39	3.19	1.50	0.12	0.20

wt pct	Mn	Si	P	S	B	Cu	C
Alloy 718	0.11	0.07	0.008	0.00001	0.003	0.09	0.015
Alloy 945X	0.07	0.06	0.010	0.00001	0.002	1.94	0.008

The heat treatments selected for the HE study were 750 °C for 6, 12, and 20 h and 730 °C for 6, 12, and 20 h for Alloy 718 and 732 °C for 6, 12, and 20 h for Alloy 945X.

1. *How does a small amount of δ phase precipitation affect the HE susceptibility of Alloy 718?*

To determine the effect of a small amount of δ phase, Alloy 718 conditions were heat treated to a series of industrially-relevant conditions with similar hardness that spanned the δ precipitation threshold.

2. *How does $M_{23}C_6$ affect the HE susceptibility of Alloy 945X?*

To study the effect of $M_{23}C_6$ in Alloy 945X, a series of industrially-relevant heat treatment conditions that spanned the $M_{23}C_6$ precipitation threshold were prepared with similar hardness.

3. *How does the HE sensitivity to δ phase precipitation in Alloy 718 compare to the HE sensitivity to $M_{23}C_6$ in Alloy 945X?*

The δ-free Alloy 718 conditions and $M_{23}C_6$-free Alloy 945X conditions underwent similar heat treatments and exhibited similar HE susceptibilities. The alloys exhibited similar increases in HE susceptibility for the conditions containing δ and $M_{23}C_6$ precipitates.

4. *Can the HE susceptibility be correlated to hydrogen-free mechanical properties?*

Charpy impact toughness, tensile, and hardness testing were conducted for each condition to relate the ambient mechanical properties to the HE susceptibility.

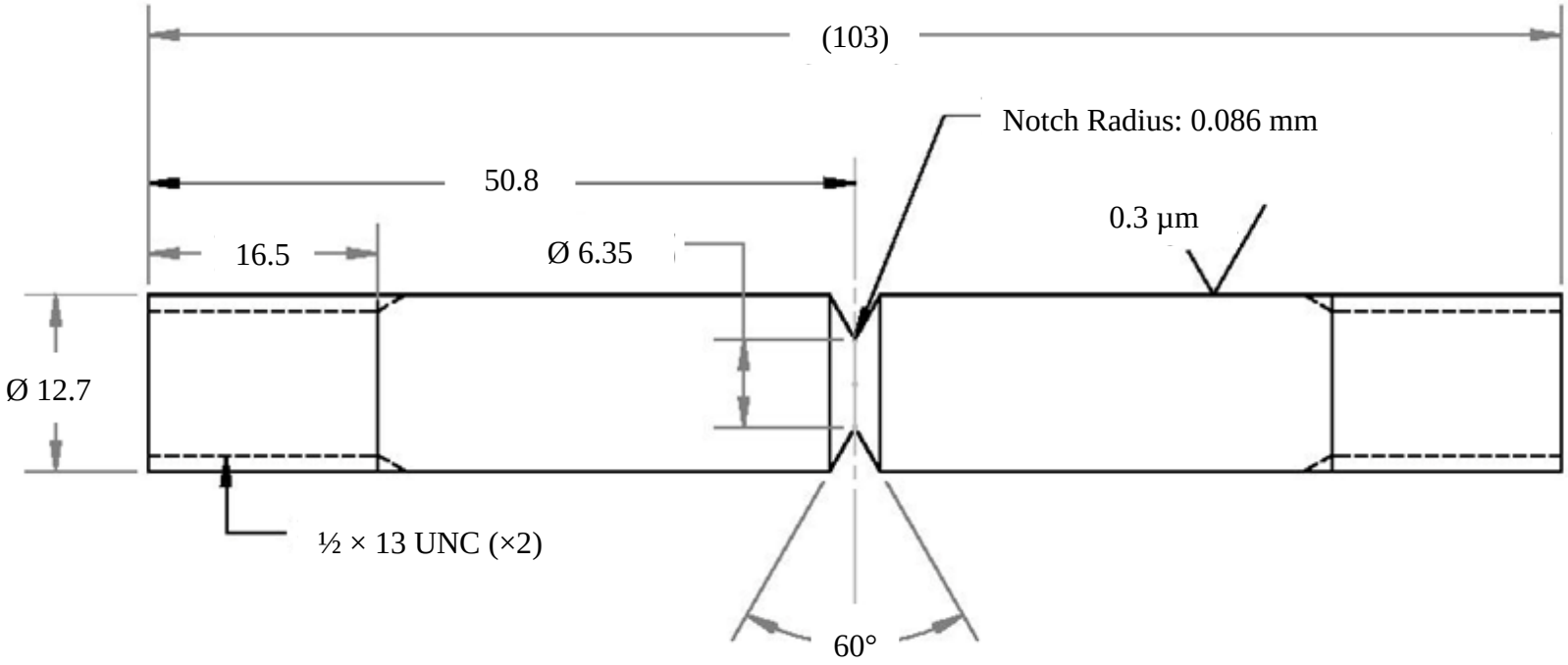

Figure 3.1 CNT drawing used for ISL testing specimens, with dimensions in millimeters and the notch root radius specified.

3.10 Coauthor Contributions

John Doe of NASA aided in data collection and analysis in Section 3.7. Jane Collaborator of NREL led the analysis described in Section 3.9.

REFERENCES

1 H. L. Eiselstein and D. J. Tillack, "The Invention and Definition of Alloy 625," *Superalloys 718, 625, and Various Derivatives,* pp. 1-14, 1991.

2 T. Smithson, "HPHT Wells," *Oilfield Review,* 2016.

3 J. J. Debarbadillo and S. K. Mannan, "Alloy 718 for Oilfield Applications," *Journal of Materials,* vol. 64, no. 2, pp. 265-270, 2012.

4 S. S. Shademan, J. W. Martin, and A. P. Davis, "UNS N07725 Nickel Alloy Connection Failure," *NACE - International Corrosion Conference Series,* vol. 1, pp. 334-356, 2012.

5 "Addendum 3 to API Standard 6ACRA, Age-hardened Nickel-based Alloys for Oil and Gas Drilling and Production Equipment," *American Petroleum Institute,* 2019.

6 D. D. Keiser and H. L. Brown, *A Review of the Physical Metallurgy of Alloy 718,* Idaho National Engineering Laboratory, Idaho Falls, ID, pp. 2-11, 1976.

7 S. Mannan, "Alloy 945X TTT Diagram," Special Metals Corporation, Personal Communication, 2019.

8 G. E. Dieter, *Mechanical Metallurgy,* 3rd ed., New York, NY: McGraw-Hill, 1986.

9 B. Kagay, "Hydrogen Embrittlement Assessment of Alloy 718 with Precipitate Variations," PhD Thesis, Colorado School of Mines, Golden, CO, 2019.

10 ASTM Standard G129-00:2013, "Standard Practice for Slow Strain Rate Testing to Evaluate the Susceptibility of Metallic Materials to Environmentally Assisted Cracking," *ASTM International,* pp. 1-7, 2013.

11 Z. Pilkey, Walter D. Pilkey, Deborah F. Bi, *Peterson's Stress Concentration Factors,* 4th ed., Hoboken, NJ: John Wiley and Sons, 2020.

APPENDIX A
SUPPLEMENTAL FILES

A.1 Coauthor Permissions

Permission to include Chapter 3 as part of this thesis has been obtained from coauthors who are not on the thesis committee; emails containing the permission statements may be found in Supplemental File CoauthorPermissionsThesis2022.docx.

Permission to include Figures and Tables reproduced from other published sources is included in Appendix B.

A.2 Supplemental Data

The full dataset referenced in Chapter Z may be found in Supplemental File CorrosionData2022.xlsx.

APPENDIX B

COPYRIGHT PERMISSIONS

Permission to include previously published material in this thesis is below. [Note to Mines student readers: these permission statements include both actual examples and examples that have been modified to illustrate common scenarios for which permission to reproduce previously published material may be required.]

1) Permission from B. Kagay regarding the reproduction of Figure 2.4(a), Figure 3.4(a), and Figure 3.5 from his thesis, Reference 9, is expressed below.

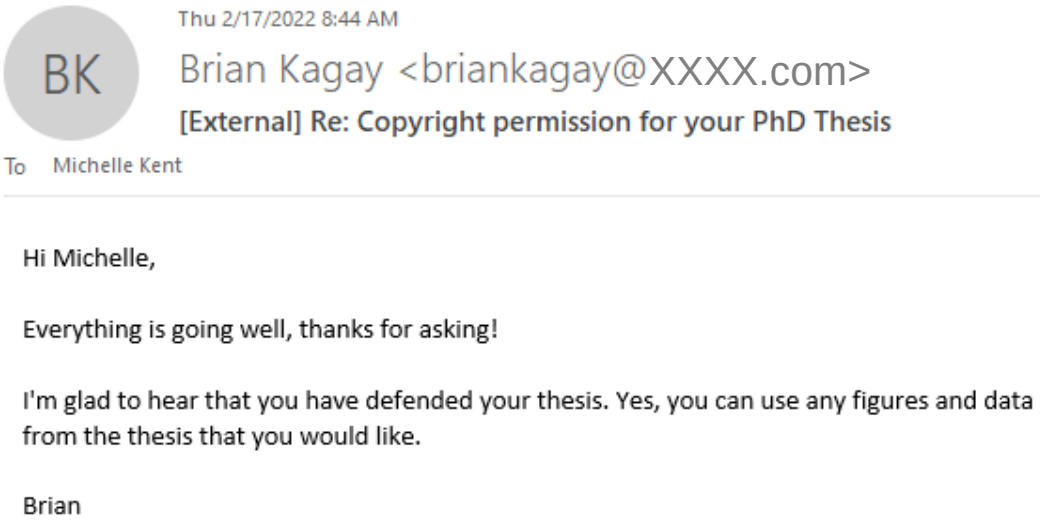

Thu 2/17/2022 8:44 AM

BK

Brian Kagay <briankagay@XXXX.com>

[External] Re: Copyright permission for your PhD Thesis

To Michelle Kent

Hi Michelle,

Everything is going well, thanks for asking!

I'm glad to hear that you have defended your thesis. Yes, you can use any figures and data from the thesis that you would like.

Brian

2) Permission from John DeBarbadillo on behalf of Special Metals regarding Figure 1.2(b), Figure 2.5, Figure 3.2(b), and Figure 3.3(b) is expressed below.

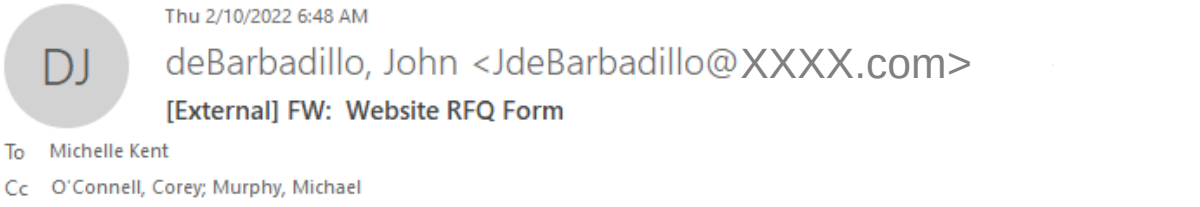

3) Copyright permission from Elsevier, the publisher of *The Journal of Abridged Theses,* is not required for the inclusion of Chapter 3 from *The Journal of Abridged Theses.* Elsevier's policy states that "Authors can include their articles in full or in part in a thesis or dissertation for non-commercial purposes." (https://www.elsevier.com/about/policies/copyright/permissions) The content in Chapter 3 is reprinted from the article cited below:

M. Kent and K. Findley, "Effect of δ Phase on the Hydrogen Embrittlement Susceptibility of Alloy 718," *Journal of Abridged Theses,* vol. 543, no. 2, pp. 119-127, 2022.

4) Figure 4.7 is reprinted from the *Journal of Sample Articles*, Vol. 1, John Doe, "Hydrogen Embrittlement: A Short Review," 100-120, (2014), used with the following permission from the publisher, SampleJournalPubCo:

SAMPLEJOURNALPUBCO LICENSE
TERMS AND CONDITIONS
Feb 10, 2022

This Agreement between Colorado School of Mines -- Michelle Kent ("You") and SampleJournalPubCo ("SJPC") consists of your license details and the terms and conditions provided by SJPC and Copyright Clearance Center.

License Number	XXXXXXXXXX
License date	Feb 09, 2022
Licensed Content Publisher	SampleJournalPubCo
Licensed Content Publication	Journal of Sample Articles
Licensed Content Title	"Hydrogen Embrittlement: A Short Review"

Licensed Content Author	J. Doe
Licensed Content Date	Feb 15, 2014
Licensed Content Volume	1
Licensed Content Issue	n/a
Licensed Content Pages	20
Start Page	100
End Page	200
Type of Use	reuse in a thesis/dissertation
Portion	figures/tables/illustrations
Number of figures/tables/illustrations	1
Format	both print and electronic
Are you the author of this SJPC article?	No
Will you be translating?	No
Title of your publication	HYDROGEN EMBRITTLEMENT IN NICKEL-BASED ALLOYS: AN ABRIDGED SAMPLE THESIS TO ILLUSTRATE FORMATTING GUIDELINES
Institution name	Colorado School of Mines
Expected presentation date	Feb 2022
Portions	Figure 4
Requestor Location	Colorado School of Mines 18575 W 59th Dr GOLDEN, CO 80403 United States Attn: Colorado School of Mines
Publisher Tax ID	
Total	0.00 USD
Terms and Conditions	

SampleJournalPubCo hereby grants you permission to reproduce the aforementioned material subject to the terms and conditions indicated.